AD NUMBER
AD842354
LIMITATION CHANGES

TO:

Approved for public release; distribution is unlimited.

FROM:

Distribution authorized to U.S. Gov't. agencies and their contractors; Critical Technology; SEP 1968. Other requests shall be referred to Air Force Technical Application Center, Washington, DC. This document contains export-controlled technical data.

AUTHORITY
usaf ltr, 25 jan 1972

AD842354

LONG-PERIOD SIGNAL SEPARATION

Special Scientific Report No. 23
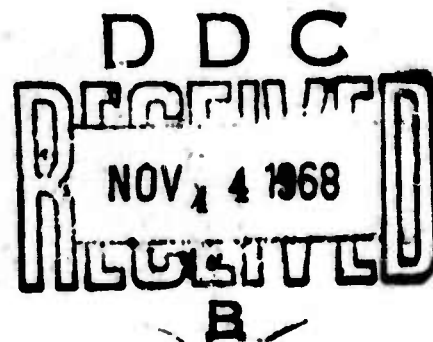LARGE-ARRAY SIGNAL AND NOISE ANALYSIS

Prepared by

Leo N. Heiting

Frank H. Binder, Program Manager
1-214-238-3473

TEXAS INSTRUMENTS INCORPORATED
Science Services Division
P.O. Box 5621
Dallas, Texas 75222

DDC
RECEIVED
NOV 4 1968
B

Contract No. AF 33(657)-16678

Prepared for

AIR FORCE TECHNICAL APPLICATIONS CENTER
Washington, D.C., 20333

Sponsored by

20 September 1968

LONG-PERIOD SIGNAL SEPARATION

Special Scientific Report No. 23
LARGE-ARRAY SIGNAL AND NOISE ANALYSIS

Prepared by

Leo N. Heiting

Frank H. Binder, Program Manager
1-214-238-3473

TEXAS INSTRUMENTS INCORPORATED
Science Services Division
P. O. Box 5621
Dallas, Texas 75222

20 September 1968

ABSTRACT

The problem of extracting the Rayleigh phase of an event of interest from a time-overlapping Rayleigh phase of another event was studied. Various configurations of the long-period LASA sensors and the following processing schemes were investigated:

- Beamsteer processing using the great circle route and the dispersion curve velocity occurring at the peak power frequency

- Wiener signal-extraction multichannel-filter processing

- A nonconventional adaptive filter processing scheme

The following conclusions are based on the results of this work:

- Current frequency-wavenumber spectral techniques are not useful in providing location information needed for processor design

- Despite the appreciable differences in waveform as seen across the array, neither the beamsteer nor MCF processors introduce serious distortion of the target event

- As expected, suppression of the interfering event becomes less as the azimuthal separation between events is reduced (best suppression achieved: $\Delta=55°$, 18 db; $\Delta=28.2°$, 12 db)

- The MCF processor is as much as 12 db superior to the beamsteer processor in suppressing the interfering event

- Multichannel filtering of small-array configurations such as the A0 and D ring or A0 and C ring is the most effective processing method of those considered

- The nonconventional adaptive processor is not effective in solving this problem

TABLE OF CONTENTS

ILLUSTRATIONS

TABLES

science services division

SECTION I
INTRODUCTION

Various methods were studied for separating Rayleigh waves from two distinct epicenters received simultaneously by a long-period array. The problem was treated in an off-line context; thus, it is assumed that both events have been detected and located by other means. The problem is to process the received data so that one event is adequately suppressed for those parameters useful for classifying the other event to become available.

The usefulness of various types of frequency-wavenumber (f-$\vec{k}$) spectra in accurately determining the apparent locations of the two events in wavenumber space is detailed in Section II. Knowledge of the apparent event locations is important in cases where significant lateral refraction of the surface waves occurs and the great circle route becomes a poor estimate of the propagation vector. In Sections III and IV, details of the following three types of signal processors are presented:

- Beamsteer processing using the great circle route and the dispersion curve velocity occurring at the peak power frequency

- Wiener signal-extraction multichannel filter processing

- A nonconventional adaptive filter processing scheme

At the time this work was performed, time-overlapping events were not available. Simulation of the problem was accomplished by compositing individual Rayleigh-wave arrivals. Pertinent details of the events used are given in Table I-1.

science services division

Table I-1

EVENT DATA

Region	Date	Origin Time (GMT)	Latitude (°)	Longitude (°)	Depth (km)	Magnitude	Δ (°)	Azimuth (°)
New Hebrides Islands	11/23/66	02:19:13.8	14.9S	166.9E	48	5.6	98.6	257.5
Hokkaido, Japan	11/12/66	12:49:43.6	41.8N	144.1E	33R	5.8	72.7	312.5
Mongolia	1/20/67	01:57:23.1	48.0N	102.9E	33	6.1	82.3	340.7
California	11/11/66	18:21:05.0	40.3N	127.1W	33R	4.5	16.4	254.6
Greenland Sea	11/18/66	18:48:43.9	73.4N	6.8E	33R	4.9	51.9	19.7

SECTION II
ESTIMATION OF EVENT VELOCITY USING FREQUENCY-
WAVENUMBER SPECTRA

The various types of MCF processors required for separating overlapping Rayleigh-wave events require modeling of either one or both interfering events. This necessitates knowing accurately the events' velocity and direction of propagation. Using the great circle route from epicenter to array for direction and the best current estimates of dispersion curves in the vicinity of the array for velocity is the most straightforward approach. However, it is well known that lateral refraction of Rayleigh waves occurs. Consequently, the straightforward estimate of event location in frequency-wavenumber space may be a poor one. It will be shown later in this report, for example, that the apparent propagation vector at LASA for one event originating in California differs by about 5° from the great circle path.

The usefulness of various types of f-$\vec{k}$ spectra in obtaining better location estimates was investigated. Events from California and Greenland were composited to simulate overlapping events; approximate Greenland-to-California amplitude ratios of 2:1, 5:1, and 10:1 were used. The following types of f-$\vec{k}$ spectra were computed for each of the three composite ratios:

- Conventional - conventional f-$\vec{k}$ spectra
- HR 1 - high-resolution f-$\vec{k}$ spectra with the A0 sensor used as reference
- HR 2 - high-resolution f-$\vec{k}$ spectra with the F-ring sensors used as reference

Analytic details of these techniques are reported in Special Scientific Report No. 2.[1] The f-$\vec{k}$ spectra were calculated at 0.04 Hz which is near the peak of the single-channel power-density spectra for both of these events. The composite-event time gate used for calculating the f-$\vec{k}$ spectra was 330 sec and contained most of the signal energy for both events.

Proper evaluation of the f-$\vec{k}$ spectral techniques requires accurate knowledge of the apparent f-$\vec{k}$ space location of the events as they propagate across the array. Table II-1 lists two different reference estimates of these locations as well as those obtained from the various f-$\vec{k}$ spectra. The computer program used in generating these spectra outputs in the form of relative db power levels at various points in wavenumber spaces as defined by a linear rectangular grid. The grid consists of 59 locations in the y direction and 49 locations in the x direction, both beginning in the lower left-hand corner. The locations in Table II-1 are given in terms of these coordinates. The first estimate was obtained using the great circle routes from the PDF epicenters to the array and the phase velocity from a LASA dispersion curve at 0.04 Hz (first line, Table II-1). The second estimate was obtained from a previous study of these two events aimed at experimental determination of the LASA Rayleigh-wave dispersion curve.[2] This work provided estimates of the velocity and direction for both of these events using various 3-sensor combinations from the LASA. The apparent f-$\vec{k}$ space locations for the two events have been visually estimated from these results and are given in the second line of Table II-1. The two estimates of the Greenland location are in relatively close agreement, but the apparent California direction departs significantly from the great circle route.

Examples of the contoured f-$\vec{k}$ spectra obtained are given in Figure II-1. These are the three different types of f-$\vec{k}$ spectra for the composite event using a 2:1 amplitude ratio. The location of peak power is indicated by a plus (+) sign, and the contours give power levels in db relative to this peak power.
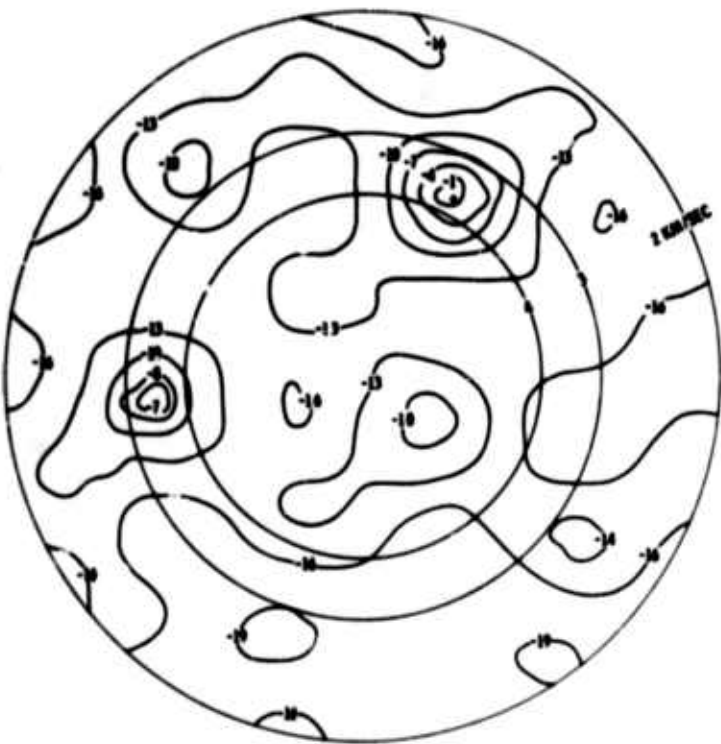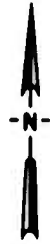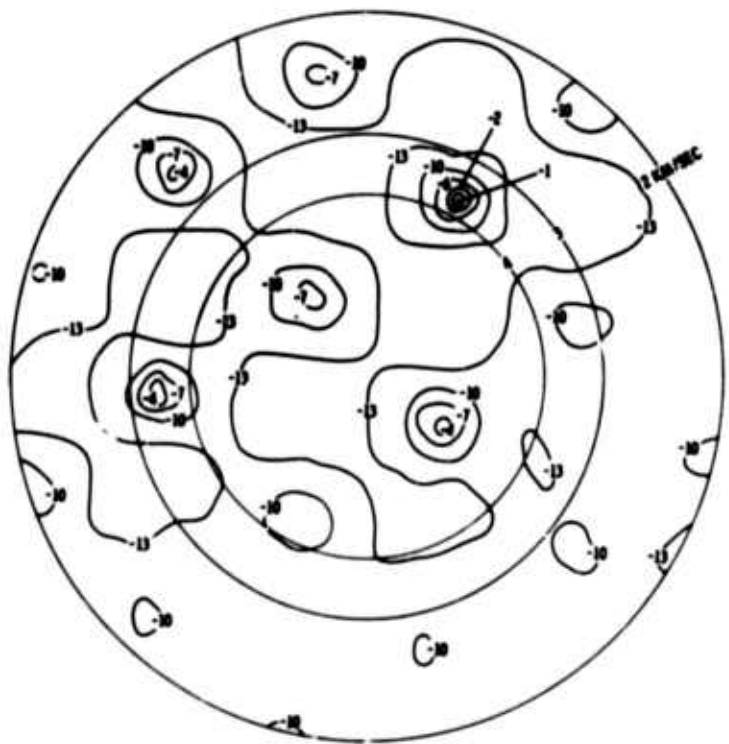
Table II-1

FREQUENCY-WAVENUMBER SPECTRA RESULTS

Method	Location of Peak Frequency				Remarks
	California		Greenland		
	k_x	k_y	k_x	k_y	
Theoretical Estimate	12.34	25.80	29.42	44.95	Velocity from LASA-North dispersive curve; 3.65 km/sec Direction from great circle route to PDE epicenter from A0: California = 254.65°, Greenland = 19.65°
Tripartite Estimate	12.22	27.00	29.33	44.7	Velocity and direction from tripartite estimates: California, V = 3.68 km/sec, θ = 259°; Greenland, V = 3.72 km/sec, θ = 19.65°
Conventional	11	28	31	44	Amplitude Ratio: Greenland/California = 2:1
HR1	11	28	31	44	
HR2	11	28	31	44	
Conventional	10	29	30	45	Amplitude Ratio: Greenland/California = 5:1
HR1	9	28	31	45	
HR2	11	29	30	45	
Conventional	9	29	30	45	Amplitude Ratio: Greenland/California = 10:1
HR1	9	28	31	45	
HR2	10	30	30	45	

CONVENTIONAL

MR1

MR2

Figure II-1. Three Types of f-$\vec{k}$ Spectra for the 2:1 Amplitude Ratio

As expected, the location of peak power on all the f-$\vec{k}$ spectra is near the larger of the two events (Greenland). Estimates of the Greenland location (listed in Table II-1) are these peak-power locations. Assuming that the reference estimates of the Greenland event are correct, the conventional and HR2 spectra properly locate this event for ratios of 5:1 and 10:1. For a ratio of 2:1, the Greenland event is improperly located by all three types of f-$\vec{k}$ spectra. For all three types of spectra, the presence of a relatively strong secondary event distorts the location of the strongest event.

In all the spectra computed, a secondary peak occurs in the vicinity of the California location. Since the computer program does not provide the coordinate where the largest value of this peak occurs, the coordinate nearest its center was selected as the California estimate. These estimates differ seriously from either reference location and must be considered erroneous.

If the problem is to extract a small event from a much larger interfering event, the results imply the following conclusions.

- It is probably possible to obtain a good estimate of the wavenumber location for the large event using conventional or HR2 spectra

- If severe lateral refraction of the event has occurred, this estimate will be superior to the great circle estimate

- It does not appear possible with any of these techniques to obtain an accurate estimate of the weak-event location

In Section III it is seen that the best MCF results are obtained by using measured data to characterize the large interfering event and by modeling the small event. Therefore, accurate location of the large event in the f-$\vec{k}$ space is of little value. In view of this, it appears that none of these f-$\vec{k}$ spectra contribute significantly to solving the interfering-event problem.

science services division

BLANK PAGE

SECTION III
EVENT SEPARATION USING BEAMSTEER AND MCF PROCESSORS

For the work discussed in this section, it is assumed that the Rayleigh wave from a large natural event has been received and that the Rayleigh wave from an event of interest has been received simultaneously. It is assumed that both events have been detected and that their epicenters have been located by other means. The problem is to suppress the interfering event sufficiently to determine classification parameters of the event of interest.

This problem has been studied using two types of processors: time-shift-and-sum and conventional MCF. A third approach is discussed in Section IV of this report. Specific questions to be answered here are as follows:

- How do the two approaches compare?
- How does performance depend on the azimuthal separation of the two events?
- What configuration of the LASA long-period sensors works best?
- How much suppression of the interfering event can be achieved using these methods?

At the time this processing began, no known instances of over-lapping long-period events existed in the available data library. To simulate the problem, therefore, it was necessary to scale and add individual events. Pertinent details of the events used are given in Table I-1. The first composite event studied consists of the interfering Hokkaido event and the target New Hebrides event with an azimuthal separation of 55°. Before adding these t/o events, the New Hebrides data was scaled down to make the peak power level of its A0 seismometer output 17 db below that for the Hokkaido event.

Since both the beamsteer and MCF processors were linear and the "signal" and "noise" events were available individually, evaluation of the processors consisted of applying the processors to the uncomposited individual events. This allowed a more precise estimate of the processors' performance. Outputs of various beamsteer processors for the New Hebrides event were illustrated in Special Scientific Report No. 20.[3] A surface-wave velocity of 3.5 km/sec was used in computing all beamsteer time delays in this section. In view of the New Hebrides event's variability, as recorded by the various vertical sensors, these results show a surprisingly small degree of signal degradation. The result of steering various combinations of the Hokkaido traces, using the New Hebrides azimuth, is shown in Figure III-1. Note that all New Hebrides traces have been scaled up by a factor of five in this figure for clarity in the display. Despite the large azimuthal separation of these two events, the best beamsteer processor provides only 6 db suppression of the peak value of the interfering wave.

Two approaches were considered when designing the MCF processors. In one case, both the signal and noise correlation matrices were obtained from theoretical dispersive plane-wave models propagating along the great circle paths to LASA from New Hebrides and Hokkaido, respectively. The frequency-dependent propagational velocities used in the models were those of the LASA-North dispersion curve.[2] The single-sensor power-density spectrum for both models had the shape given in Figure III-2. This was chosen to force the MCF's to work in the frequency range where signal and noise power are known to exist. A signal-to-noise ratio of approximately 4 was used in all MCF designs. Two theoretical MCF processors were designed for the New Hebrides-Hokkaido composite, one employing the A0 and C-ring verticals and the other employing the A0 and E-ring verticals.
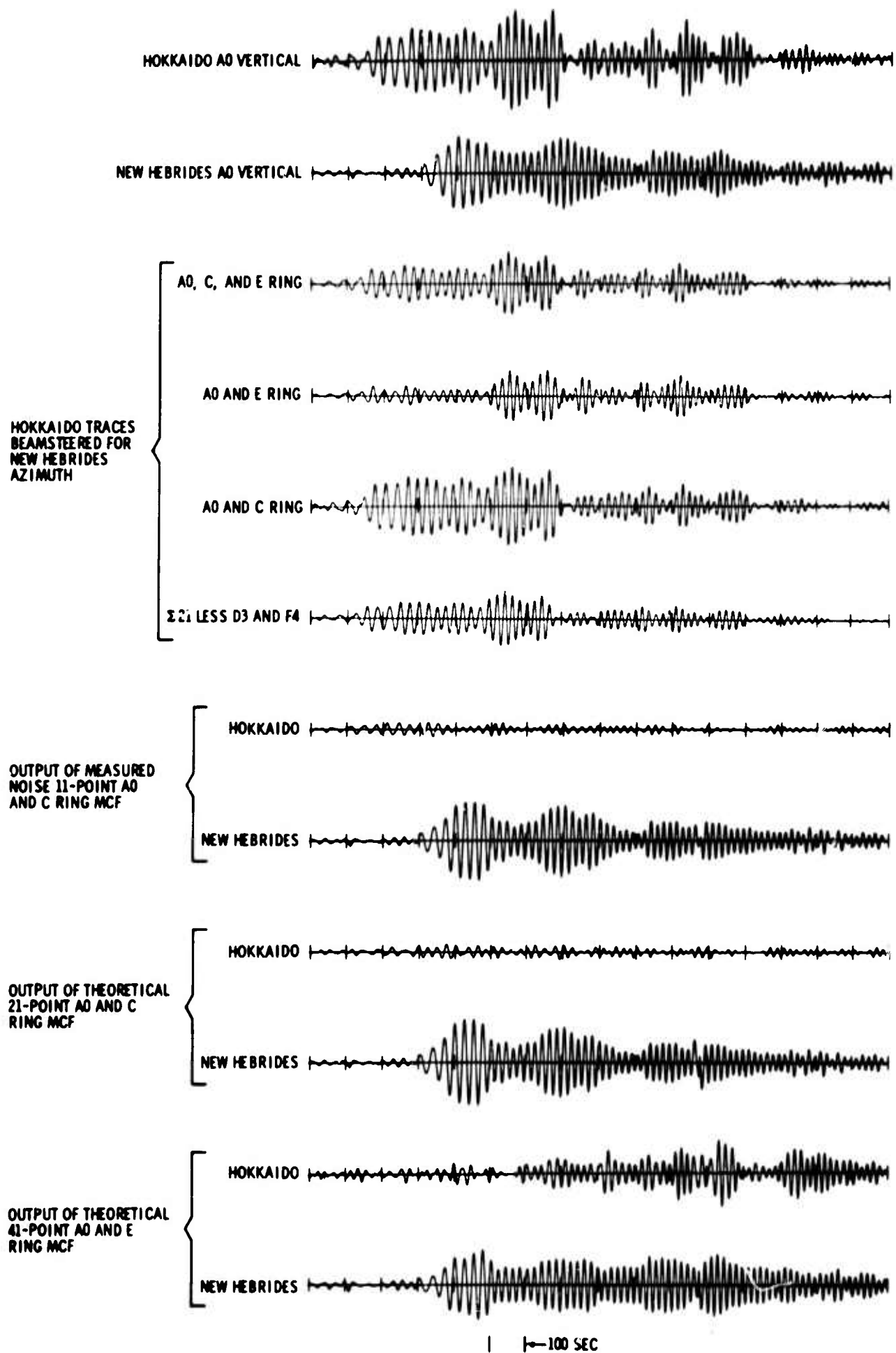
Figure III-1. New Hebrides — Hokkaido Processing Results
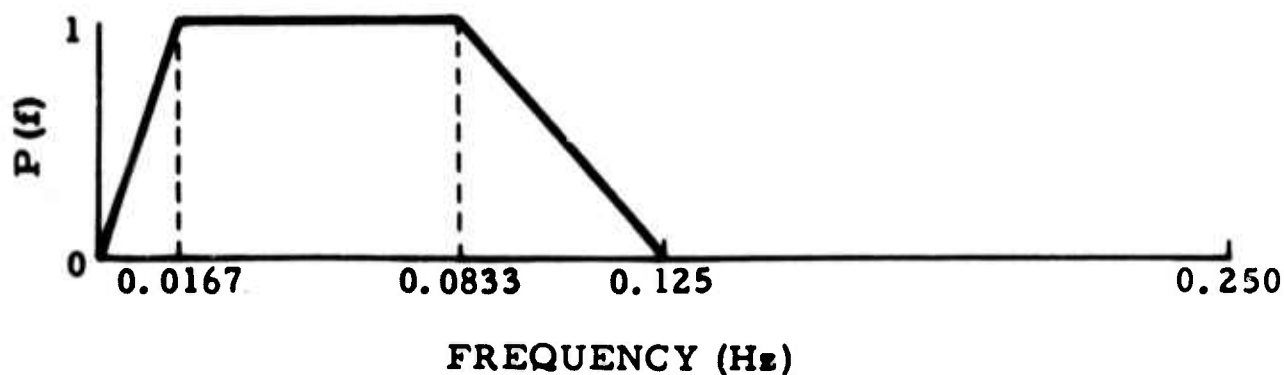
science services division

Figure III-2. Theoretical Model Power-Density Spectrum

In the second type of MCF design, a measured correlation set was obtained from the composite traces. The fact that this set contains a small amount of signal data was neglected and this set was used as the noise correlations. Signal correlations were again obtained from a theoretical model, but in this case, the single-sensor power-density spectrum was given the same shape as the A0 sensor-measured power-density spectrum. An MCF of this type was designed for the A0 and C-ring sensors. In this design, the signal autocorrelations were scaled by 1.01 representing statistical gain fluctuation, and the zero lags of the noise autocorrelations were scaled by 1.01 representing white noise.

The results of applying these MCF processors to the individual Hokkaido and New Hebrides data sets are given in Figure III-1. Examining the data in Figure III-1 indicates that

- Neither beamsteer nor MCF processing introduces severe signal distortion

- Both A0 and C-ring MCF processors suppress the peak value of the noise by about 18 db and are significantly superior to any of the beamsteer processors in this respect

- If the A0/E-ring combination is used, neither beamsteer nor theoretical MCF processing is clearly superior

- The theoretical A0/E-ring MCF is inferior to either A0/C-ring MCF processor

Maximum-entropy power-density spectra of the MCF outputs and of the A0 Hokkaido and New Hebrides traces are illustrated in Figure III-3. The C-ring MCF's provide significant suppression of the Hokkaido event throughout the frequency range where appreciable power exists. The E-ring processor, however, is largely ineffective beyond 0.05 Hz.

Frequency-wavenumber responses of the two theoretical MCF processors are shown in Figures III-4 and III-5. Only that portion of wavenumber space which includes the apparent location of the two events is displayed. The indicated frequencies bracket the range of peak power for these events. At each frequency, the points corresponding to the velocity of the LASA-North dispersion curve and to the directions of the two events are indicated by dots. In all cases, the response is very nearly 0 db at the signal location and shows varying amounts of suppression at the noise location. At 0.07 Hz, the E-ring MCF response has a sharp gradient in the vicinity of the noise. The poor performance of this MCF is probably either due to one or a combination of two causes. In view of the sharp response gradient at 0.07 Hz, small errors in locating the noise model could result in poor suppression of the actual noise. Alternately, the wide variations in the noise waveform — as perceived by the E-ring sensors — may prevent effective MCF processing with this configuration. This approach was discarded for subsequent designs, since using a theoretical noise model allows the possibility of "missing" the actual interfering event and since comparison of the two C-ring designs shows no apparent advantage for the theoretical design.

A second composite event, having an azimuthal separation of 28.2°, was formed from the Hokkaido and Mongolia events. Again, the Hokkaido event was considered to be the interfering event, and the Mongolia data was scaled down to make its A0 seismometer peak power level 18 db below that for the Hokkaido event.

science services division

NEW HEBRIDES — HOKKAIDO

MEASURED NOISE 11-POINT A0 AND C RING MCF

THEORETICAL 21-POINT A0 AND C RING MCF

THEORETICAL 41-POINT A0 AND E RING MCF
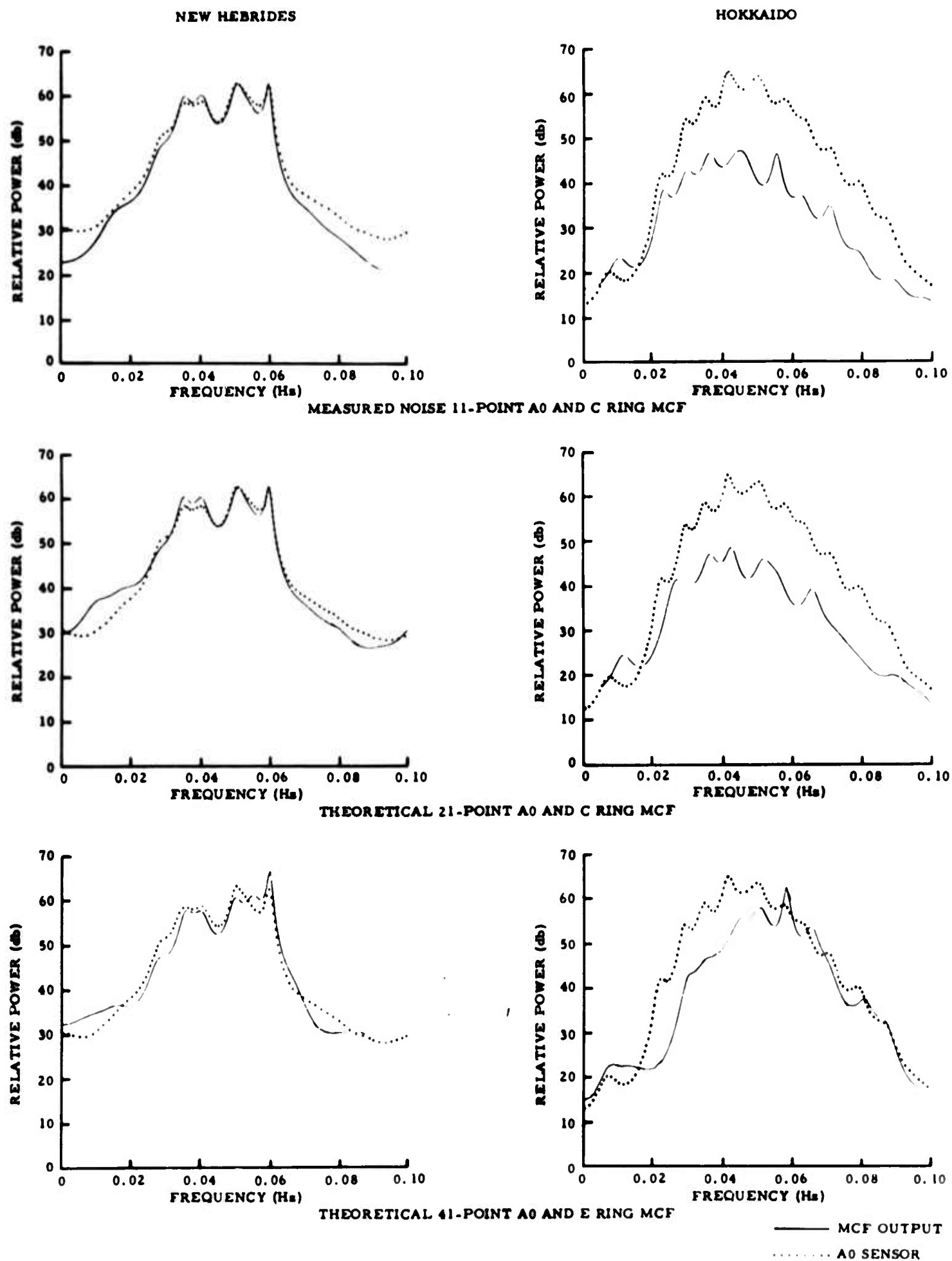
—— MCF OUTPUT
······· A0 SENSOR
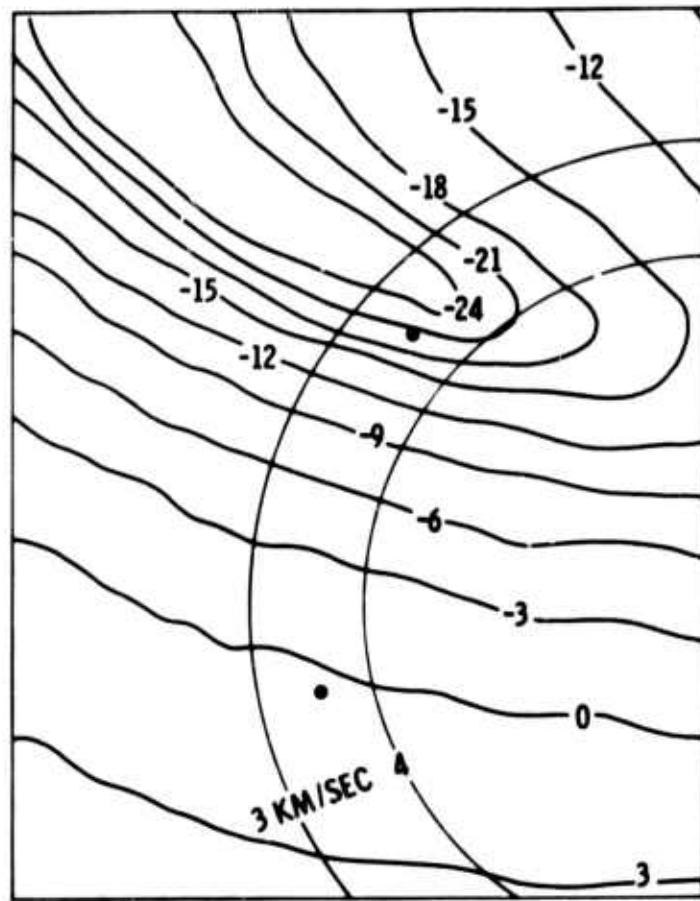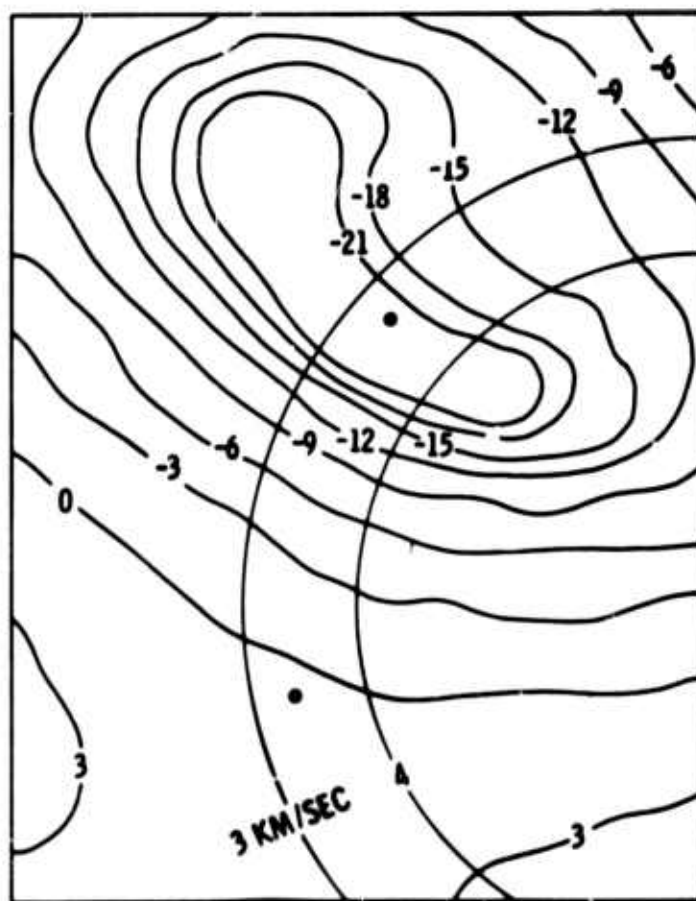
Figure III-3. Maximum-Entropy Power-Density Spectra
of MCF Outputs
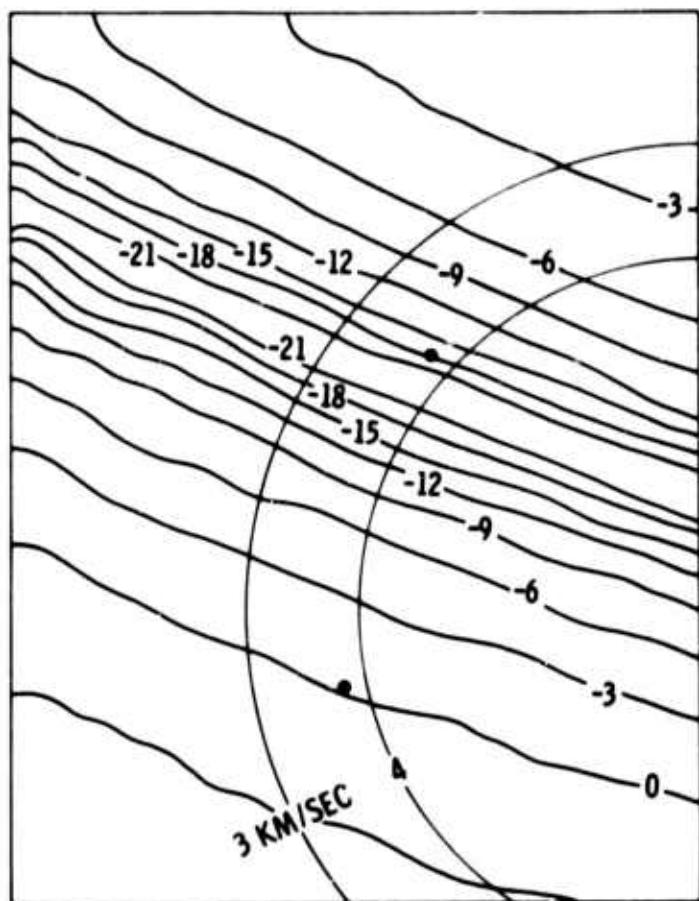
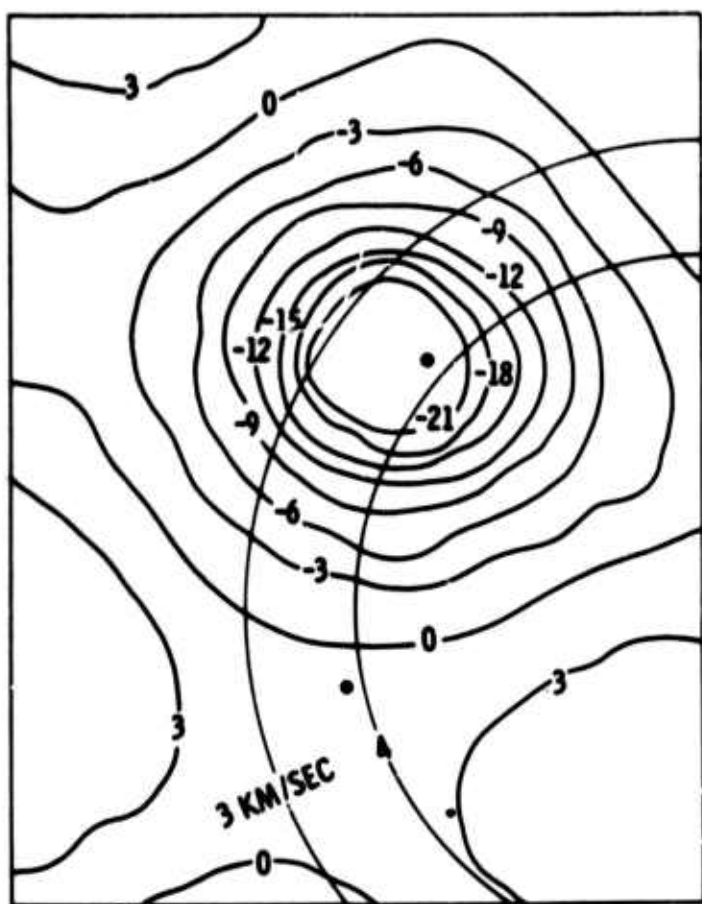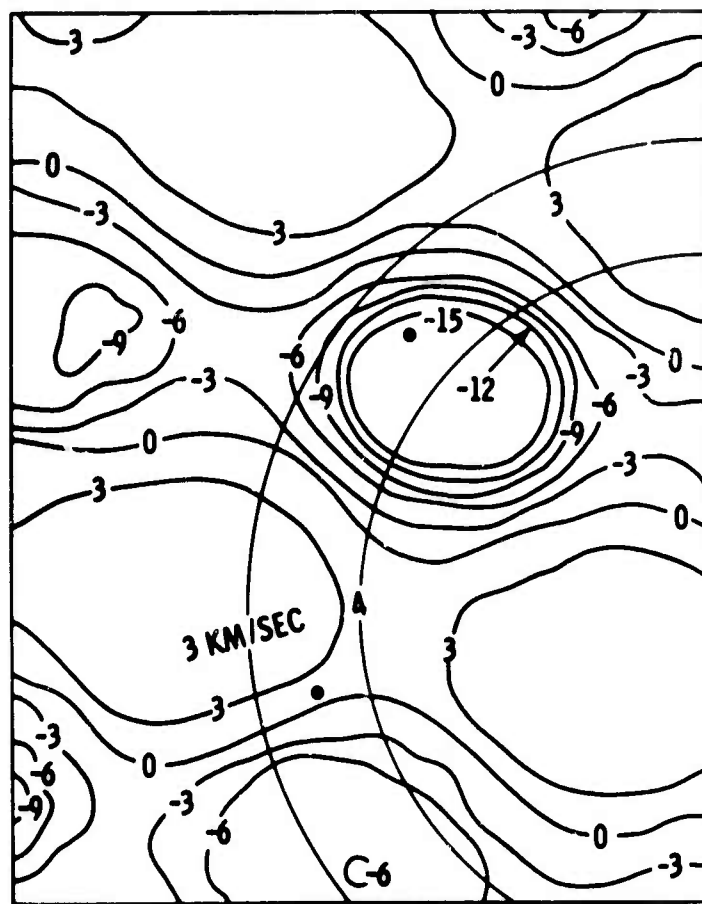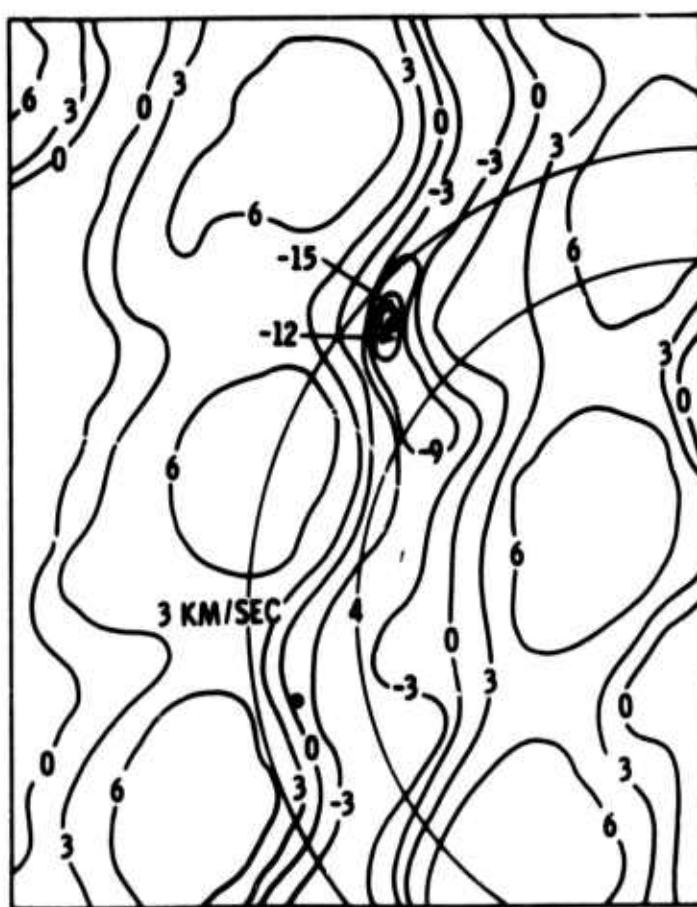Figure III-4. Wavenumber Response of C-Ring Theoretical
MCF at 0.03, 0.05, and 0.07 Hz

Figure III-5. Wavenumber Response of E-Ring Theoretical
MCF at 0.03, 0.05, and 0.07 Hz

Beamsteer outputs for the Mongolia event were illustrated in Special Report No. 20.[3] Again, signal degradation resulting from beamsteer processing is seen to be negligible. Note that about the first third of these beamsteer traces represents energy arriving prior to the onset of the Rayleigh phase. The results of using the Mongolia azimuth to steer various combinations of the Hokkaido traces are shown in Figure III-6. The best beamsteer suppresses the peak value of the interfering wave by less than 4 db.

Initially, two MCF processors were designed — an 11-point filter using the A0 and C-ring sensors and a 31-point filter using the A0 and E-ring sensors. Both statistical gain fluctuation and white noise were used in these designs. Noise and signal outputs for these processors, as well as those to be discussed below, appear in Figure III-6. A small degree of signal degradation occurs in each case. Attenuation of the interfering event by these two processors is similar and is somewhat better than that provided by any of the beamsteer processors. Nevertheless, the peak value of either MCF noise output is only about 9 db below that of the unprocessed interfering event as seen by the A0 seismometer. Apparently, the C-ring aperture is insufficient to adequately resolve these two events, while the E-ring MCF suffers from dissimilarities in the interfering event as seen by its sensors.

In an effort to permit the A0/C-Ring MCF greater latitude in working on the interfering event, the design was repeated without statistical gain fluctuation. The results in Figure III-6 show no significant improvement.

Power spectra of these three MCF outputs, along with those of the A0 Hokkaido and Mongolia traces, are shown in Figure III-7. In all cases, the peak noise suppression occurs at about 0.042 Hz. Its value is 13 db for the C-ring MCF designed with statistical gain fluctuation and 15 db for the other two designs. Average noise suppression over the 0.03- to 0.07-Hz range is somewhat less.
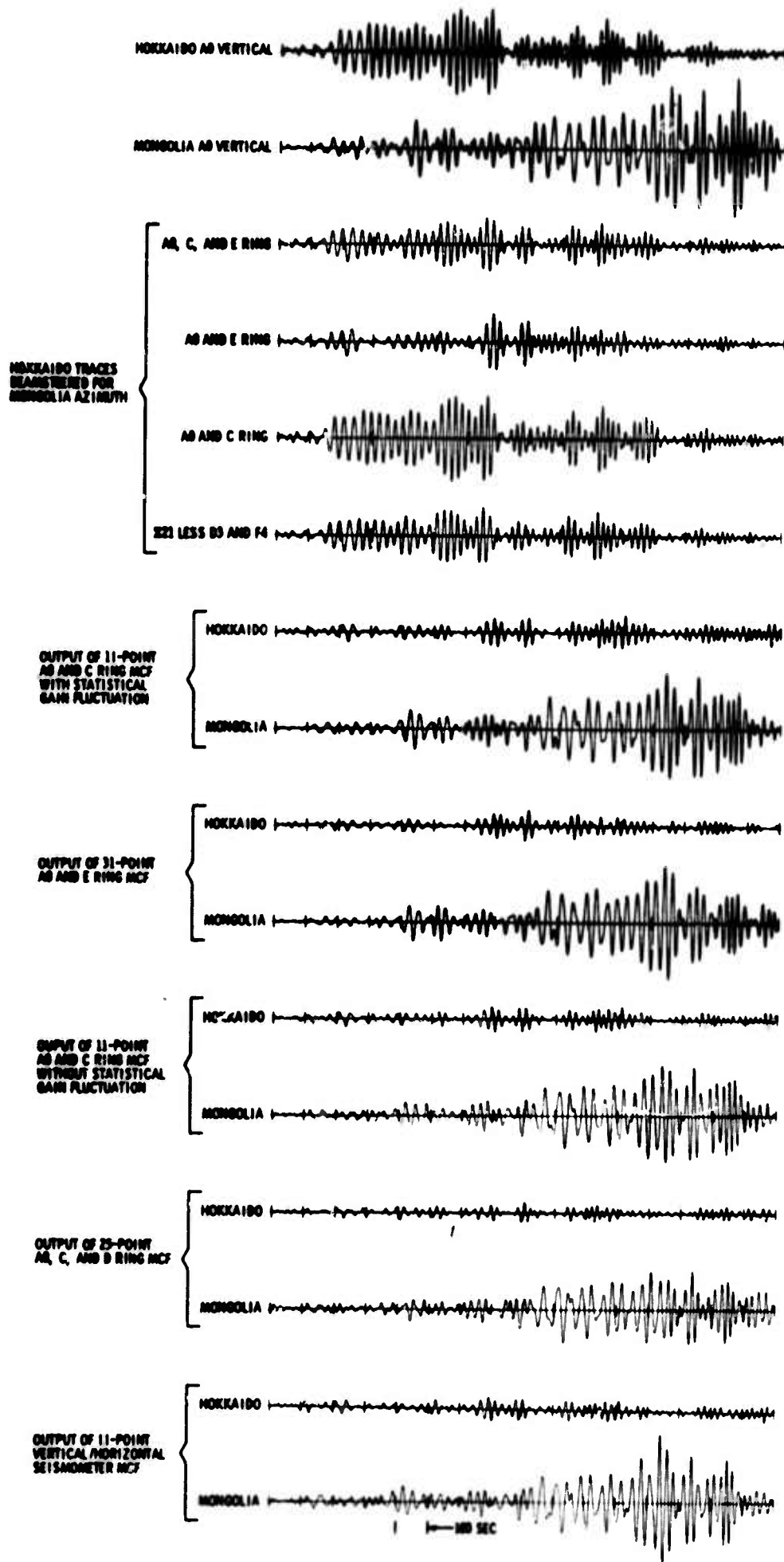
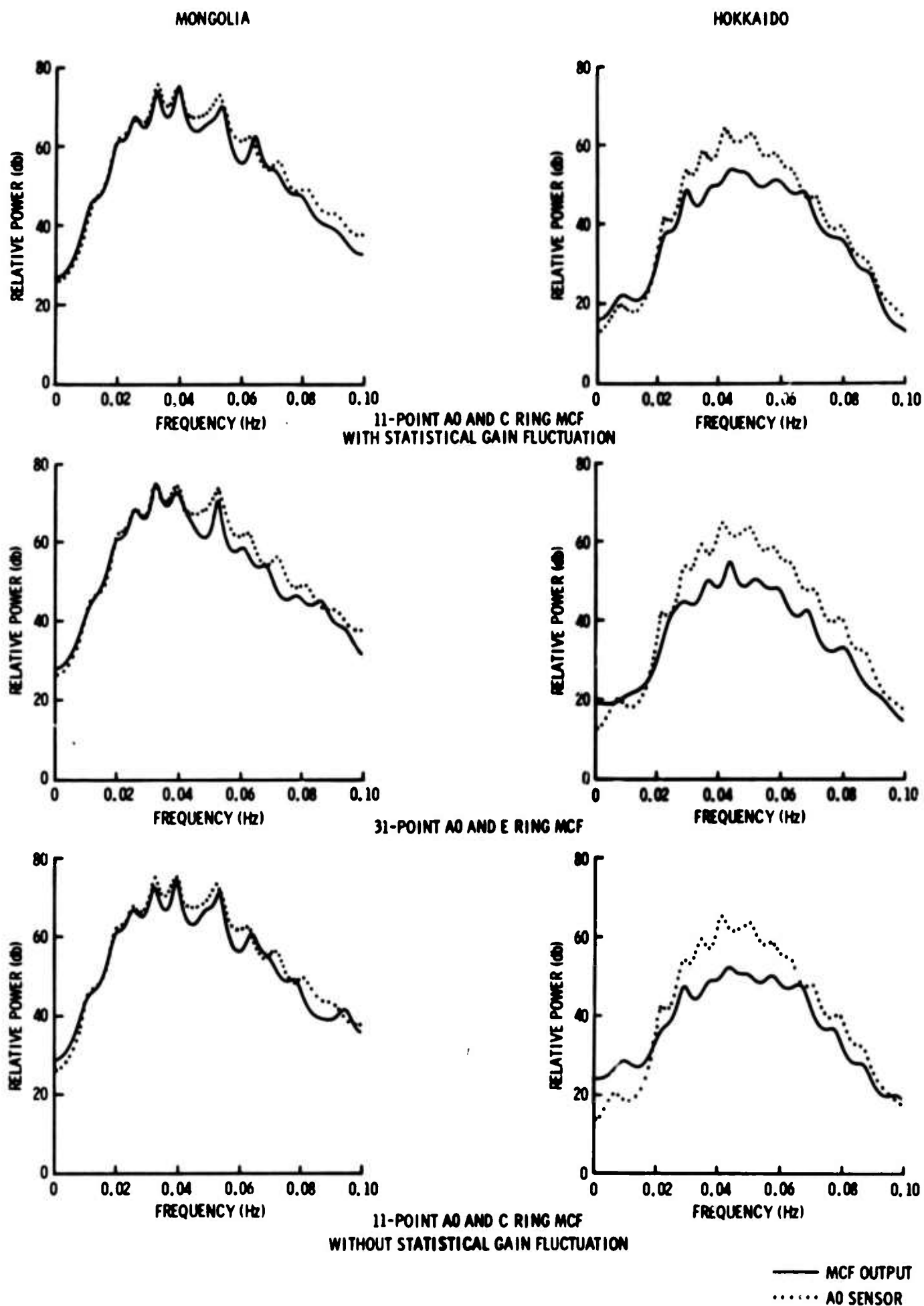Figure III-6. Mongolia – Hokkaido Processing Results

Figure III-7. Maximum-Entropy Power-Density Spectra of MCF Outputs

Two additional MCF processors were designed for this pair of events. The first was a 9-channel 25-point MCF using the A0, C-, and D-ring sensors. The second employed a combination of vertical and horizontal sensors. Before processing, the N-S and E-W horizontal traces were scaled and trigonometrically rotated to form a resultant trace which would be seen by a sensor oriented transverse to the Mongolian signal's direction of propagation. An 8-channel 11-point MCF was designed using the A0 and C-ring vertical sensors and the A0, B2, and B3 transverse horizontal sensors. (The B1 and B4 horizontal sensors were anomalous for this composite).

The 9-channel (A-, C-, and D-ring vertical sensors) processor provides only a small amount of improvement in noise attenuation and has rather severe signal degradation. The 8-channel (vertical/horizontal sensor) processor likewise suppresses the interfering event slightly better than the other processors but shows very little singal attenuation.

With the exception of the 9-channel A0, C-, and D-ring MCF, all processors studied have produced only a small amount of signal degradation. Therefore, the figure of merit used in summarizing these results will be the ratio of the peak amplitude in the processor noise output to the peak amplitude in the A0 sensor noise trace. Using this yardstick, the following conclusions can be made.

- MCF processing significantly suppresses the interfering wave better than beamsteer processing. The degree of this difference varies with the separation of events and with the sensor configuration and ranges as high as 12 db. The best MCF results are obtained by using the received composite waveforms to obtain an estimate of the noise correlation matrix for filter design.

- In comparing 5-channel MCF processors, the A0/ C-ring combination appears to work as well or better than the A0/E-ring. Upon adding D-ring sensors to the A0, the C-ring combination substantially

increases the signal degradation. Adding several horizontal transverse sensors to the A0/C-ring combination adds slightly to the suppression capability, with no noticeable increase in signal degradation.

- The best noise suppression achieved for the events separated by 55° was about 18 db. When the event separation was 28.2°, this suppression dropped to 12 db.

BLANK PAGE

SECTION IV
SEPARATION OF EVENTS USING ADAPTIVE PROCESSING

In the ideal case, two interfering plane waves can be separated using only two channels of data. In practice, however, departures from plane-wave theory caused by such phenomena as local scattering and multipath propagation seriously hamper this simple approach. A straightforward adaptive filtering scheme has been studied in an effort to overcome these difficulties.

Again, it is assumed that two time-overlapping Rayleigh waves have been received and that the azimuth from station to epicenter for both is known. In this study, events from Greenland and California were composited, with the latter considered to be the signal. In forming the composite, the California event was scaled down to make the peak value of its A0 trace about 15 db below that of the Greenland event. The composite has two significant characteristics:

- The similarity of these events as seen by the various LASA long-period vertical seismometers is better than that observed for most Rayleigh-wave arrivals

- The azimuthal separation of these two events is approximately $125°$

As a result, this particular composite represents an unusually simple problem, and the results obtained should provide an upper performance limit for the method under study.

After forming the composite event, a beam was formed toward the Greenland epicenter using a 3.5-km/sec velocity. Presumably this beam-steer output is a good replica of the Greenland arrival and contains little

California energy. After time-shifting the individual composite traces to make their Greenland arrivals time-align with that in the beamsteer, individual short 1-channel adaptive prediction filters were designed to predict each of the traces from the beamsteer output. Ideally, each of the prediction-error traces should contain the undistorted California event and the strongly attenuated Greenland event. Finally, the prediction-error traces were beamsteered for the California azimuth to further suppress the remaining Greenland energy.

The adaptive algorithm used in designing the single-channel prediction filters was given previously and is repeated here.[4]

$$\epsilon_n = y_n - F_n^T X_n$$

$$F_{n+1} = F_n + 2k_s \epsilon_n X_n$$

where

y_n is the nth data point in the trace to be predicted

X_n is an N x 1 column vector containing the N points of the beamsteer output used in predicting y_n

F_n is an N x 1 column vector containing the N filter weights used in predicting y_n

ϵ_n is the error in predicting y_n

k_s is a convergence parameter determining the rate of filter adaptation

Widrow has shown that, for an N-point adaptive filter which predicts a time-series data point from the preceding N data points, the following stability requirement holds for k_s:[5]

$$0 < k_s < \frac{1}{X_{jmax}^T X_{jmax}}$$

In the present case where one time series is used to predict another similar time series, a practically identical constraint is as follows:

$$0 < k_s < \frac{1}{x_{jmax}^2 (NFP)}$$

where

x_{jmax} is the maximum value of the data

NFP is the number of filter points

For the type of data used, this upper limit on k_s is conservative. Since it is desirable to have the filters adapt as rapidly as possible, the beamsteer trace is first scanned to determine x_{jmax}, and k_s is set to the upper limit. The use of short filters is necessary to permit sufficiently rapid adaptation.

The technique was first evaluated using the A0, D-, and E-ring sensors with 3-point filters. Figure IV-1 shows the A0-sensor California and Greenland traces, the nine prediction-error traces, and the final output. Note that the Greenland A0 trace has been scaled down by a factor of 10 in this display. Clipping of several of the prediction-error traces is a plotting error.

The first portion of the interfering event is attenuated by more than 30 db; however, as the event proceeds, this attenuation diminishes rapidly and only about 10-db suppression of the interfering event is observed near the end of the record. Apparently, dissimilarity in the individual seismometer outputs (which becomes more severe in the latter portion of the record) seriously hampers the single-channel filters. In addition to this limited effectiveness in suppressing the interfering event, about 6-db signal attenuation is observed.

science services division

AO CALIFORNIA

AO GREENLAND X0.1

PROCESSOR OUTPUT

E2

E1

E4

E3

D2

D1

D4

D3

AO

PREDICTION ERROR TRACES

|————— 1017 SEC. —————|
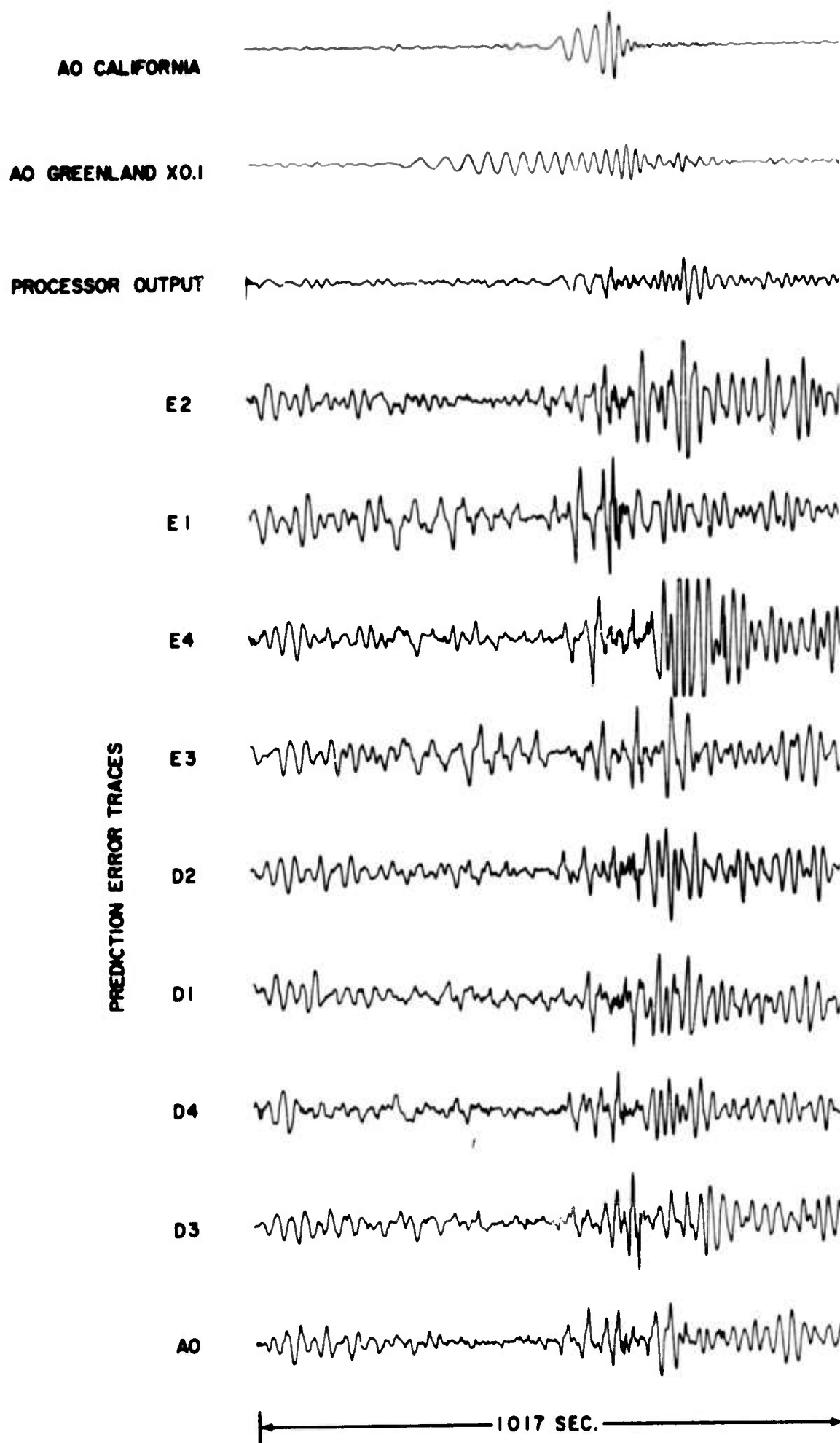
Figure IV-1. A0, D-, and E-Ring Adaptive Processor Results
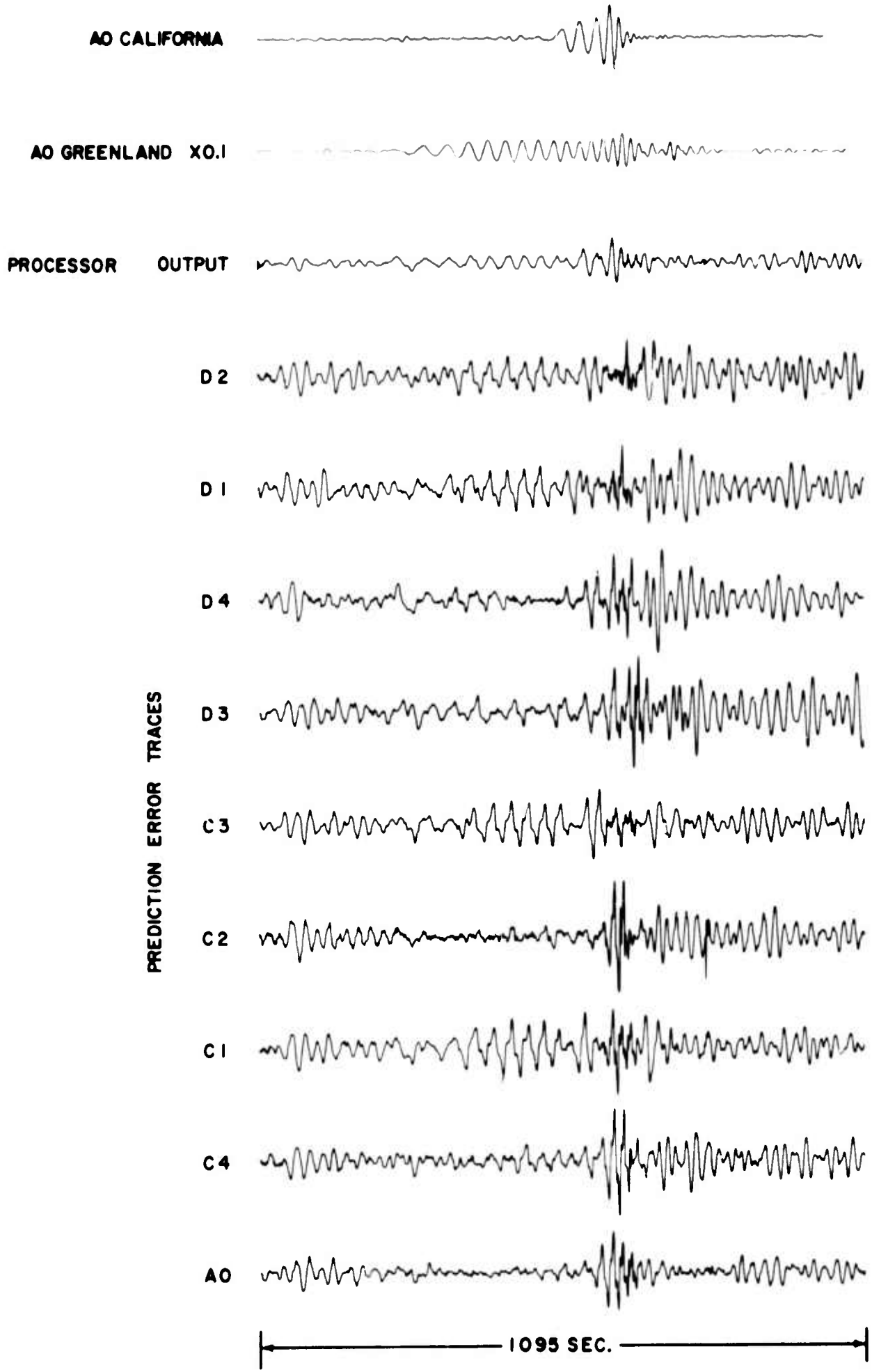
science services division

Figure IV-2. A0, C-, and D-Ring Adaptive Processor Results

In an effort to lessen the effect of signal dissimilarities, the experiment was repeated using the A0, C-, and D-ring sensors. In this case, 1-point filters were used, permitting a threefold increase in the rate of adaptation under the previously cited stability constraint. The results in this case are shown in Figure IV-2. Noise attenuation in the latter portion of the record has improved only slightly. Similarly, degradation of the signal has lessened but is still severe. In addition, suppression of the first portion of the interfering event is reduced to approximately 24 db.

Despite the relatively favorable nature of this particular compound event, the technique appears to be very limited in its ability to separate the two events. Most cases of practical interest will be less favorable, both from the standpoint of azimuthal separation and of signal dissimilarity across the array. Therefore, it is concluded that the technique is of little value for separating time-overlapping long-period Rayleigh waves.

SECTION V

CONCLUSIONS AND RECOMMENDATIONS

The following conclusions are based on the results of this work.

- Current frequency wavenumber spectral techniques are not useful in providing location information needed for processor design

- Despite the appreciable differences in waveform as seen across the array, neither the beamsteer nor MCF processors introduce serious distortion of the target event

- As expected, suppression of the interfering event becomes less as the azimuthal separation between events is reduced (best suppression achieved: $\Delta = 55°$, 18 db; $\Delta = 28.2°$, 12 db)

- The MCF processor is superior to the beamsteer processor by as much as 12 db in suppressing the interfering event

- Multichannel filtering of small-array configurations (e.g., the A0/D ring or A0/C ring) is the most effective processing method of those considered

- The nonconventional adaptive processor is not effective in solving this problem

Further study is recommended in the following areas.

- One example of the use of horizontal sensors in event separation has been investigated and further exploration seems advisable

- Applying the best processor configurations obtained in this study to a number of other overlapping events would provide a firmer estimate of the achievable performance levels

science services division

- Background noise levels in the compound events used were very low. The combined problem of extracting a Rayleigh-wave signal from a time-overlapping Rayleigh-wave signal and from ambient noise needs study

- The possibility of combining multichannel filtering and subsequent matched filtering of the MCF output may produce further gains

SECTION VI
REFERENCES

1. Texas Instruments Incorporated, 1967: Research on High-Resolution Frequency-Wavenumber Spectra, Large-Array Signal and Noise Analysis, Spec. Rpt. 2, Contract AF 33(657)-16678, 20 Apr.

2. Texas Instruments Incorporated, 1967: Continuation of Basic Research in Crustal Studies, Crustal Studies Final Rpt., Contract AF 48(638)-1588, 15 Jul.

3. Texas Instruments Incorporated, 1968: Long-Period Summation Processing, Large-Array Signal and Noise Analysis, Spec. Rpt. 20, Contract AF 33(657)-16678 (to be published).

4. Texas Instruments Incorporated, 1967: Adaptive Filtering of Seismic Array Data, Advanced Array Research, Spec. Rpt. 1, Contract F33657-67-C-0708, 18 Sep.

5. Widrow, B., 1966: Adaptive Filters, I — Fundamentals, Tech. Rpt. 6764-6, Contract DA-01-021 AMC-90015 (Y) and NOBsr-95038, Stanford Univ., Dec.

DOCUMENT CONTROL DATA · R&D

(Security classification of title, body of abstract and indexing annotation must be entered when the overall report is classified)

1. ORIGINATING ACTIVITY (Corporate author)	2a. REPORT SECURITY CLASSIFICATION
Texas Instruments Incorporated Science Services Division P.O. Box 5621, Dallas, Texas 75222	Unclassified
	2b. GROUP ————

3. REPORT TITLE

LONG-PERIOD SIGNAL SEPARATION — LARGE-ARRAY SIGNAL AND NOISE ANALYSIS — SPECIAL SCIENTIFIC REPORT NO. 23

4. DESCRIPTIVE NOTES (Type of report and inclusive dates)

Special Scientific

5. AUTHOR(S) (Last name, first name, initial)

Heiting, Leo N.

6. REPORT DATE	7a. TOTAL NO. OF PAGES	7b. NO. OF REFS
20 September 1968	32	5

8a. CONTRACT OR GRANT NO.	9a. ORIGINATOR'S REPORT NUMBER(S)
Contract No. AF 33(657)-16678	
b. PROJECT NO. AFTAC Project No. VT/6707	————
c.	9b. OTHER REPORT NO(S) (Any other numbers that may be assigned this report)
d.	————

10. AVAILABILITY/LIMITATION NOTICES

This document is subject to special export controls and each transmittal to foreign governments or foreign nationals may be made only with prior approval of Chief, AFTAC.

11. SUPPLEMENTARY NOTES	12. SPONSORING MILITARY ACTIVITY
ARPA Order No. 599	Air Force Technical Applications Center VELA Seismological Center Headquarters, USAF, Washington, D.C.

13. ABSTRACT

The problem of extracting the Rayleigh phase of an event of interest from a time-overlapping Rayleigh phase of another event was studied. Various configurations of the long-period LASA sensors and the following processing schemes were investigated: beamsteer processing using the great circle route and the dispersive curve velocity occurring at the peak power frequency; Wiener signal-extraction multichannel-filter processing; and a nonconventional adaptive filter processing scheme. The following conclusions are based on the results of this work. Current frequency-wavenumber spectral techniques are not useful in providing location information needed for processor design. Despite the appreciable differences in waveform as seen across the array, neither the beamsteer nor MCF processors introduce serious distortion of the target event. As expected, suppression of the interfering event becomes less as the azimuthal separation between events is reduced. The MCF processor is as much as 12 db superior to the beamsteer processor in suppressing the interfering event. Multichannel filtering of small-array configurations such as the A0 and D ring or A0 and C ring is the most effective processing method of those considered. The nonconventional adaptive processor is not effective in solving this problem.

DD FORM 1473
JAN 64

14.		LINK A		LINK B		LINK C	
KEY WORDS		ROLE	WT	ROLE	WT	ROLE	WT
Large-Array Signal and Noise Analysis							
LASA							
Long-Period Signal Separation							
Time-Overlapping Rayleigh Phases							
Beamsteer Processing							
Wiener Signal-Extraction Multichannel-Filter Processing							
Adaptive Filter Processing							

INSTRUCTIONS

I. ORIGINATING ACTIVITY: Enter the name and address of the contractor, subcontractor, grantee, Department of Defense activity or other organization (*corporate author*) issuing the report.

2a. REPORT SECURITY CLASSIFICATION: Enter the overall security classification of the report. Indicate whether "Restricted Data" is included. Marking is to be in accordance with appropriate security regulations.

2b. GROUP: Automatic downgrading is specified in DoD Directive 5200.10 and Armed Forces Industrial Manual. Enter the group number. Also, when applicable, show that optional markings have been used for Group 3 and Group 4 as authorized.

3. REPORT TITLE: Enter the complete report title in all capital letters. Titles in all cases should be unclassified. If a meaningful title cannot be selected without classification, show title classification in all capitals in parenthesis immediately following the title.

4. DESCRIPTIVE NOTES: If appropriate, enter the type of report, e.g., interim, progress, summary, annual, or final. Give the inclusive dates when a specific reporting period is covered.

5. AUTHOR(S): Enter the name(s) of author(s) as shown on or in the report. Enter last name, first name, middle initial. If military, show rank and branch of service. The name of the principal author is an absolute minimum requirement.

6. REPORT DATE: Enter the date of the report as day, month, year; or month, year. If more than one date appears on the report, use date of publication.

7a. TOTAL NUMBER OF PAGES: The total page count should follow normal pagination procedures, i.e., enter the number of pages containing information.

7b. NUMBER OF REFERENCES: Enter the total number of references cited in the report.

8a. CONTRACT OR GRANT NUMBER: If appropriate, enter the applicable number of the contract or grant under which the report was written.

8b, 8c, & 8d. PROJECT NUMBER: Enter the appropriate military department identification, such as project number, subproject number, system numbers, task number, etc.

9a. ORIGINATOR'S REPORT NUMBER(S): Enter the official report number by which the document will be identified and controlled by the originating activity. This number must be unique to this report.

9b. OTHER REPORT NUMBER(S): If the report has been assigned any other report numbers (*either by the originator or by the sponsor*), also enter this number(s).

10. AVAILABILITY/LIMITATION NOTICES: Enter any limitations on further dissemination of the report, other than those imposed by security classification, using standard statements such as:

(1) "Qualified requesters may obtain copies of this report from DDC."

(2) "Foreign announcement and dissemination of this report by DDC is not authorized."

(3) "U. S. Government agencies may obtain copies of this report directly from DDC. Other qualified DDC users shall request through

_____."

(4) "U. S. military agencies may obtain copies of this report directly from DDC. Other qualified users shall request through

_____."

(5) "All distribution of this report is controlled. Qualified DDC users shall request through

_____."

If the report has been furnished to the Office of Technical Services, Department of Commerce, for sale to the public, indicate this fact and enter the price, if known.

11. SUPPLEMENTARY NOTES: Use for additional explanatory notes.

12. SPONSORING MILITARY ACTIVITY: Enter the name of the departmental project office or laboratory sponsoring (*paying for*) the research and development. Include address.

13. ABSTRACT: Enter an abstract giving a brief and factual summary of the document indicative of the report, even though it may also appear elsewhere in the body of the technical report. If additional space is required, a continuation sheet shall be attached.

It is highly desirable that the abstract of classified reports be unclassified. Each paragraph of the abstract shall end with an indication of the military security classification of the information in the paragraph, represented as (TS), (S), (C), or (U).

There is no limitation on the length of the abstract. However, the suggested length is from 150 to 225 words.

14. KEY WORDS: Key words are technically meaningful terms or short phrases that characterize a report and may be used as index entries for cataloging the report. Key words must be selected so that no security classification is required. Identifiers, such as equipment model designation, trade name, military project code name, geographic location, may be used as key words but will be followed by an indication of technical context. The assignment of links, rules, and weights is optional.

GPO 886-551